Dual-responsive drug release from oligonucleotide-capped mesoporous silica nanoparticles

ARTICLE · JUNE 2013

DOI: 10.1039/C3BM60090D

3 AUTHORS, INCLUDING:

Xing Ma
Max Planck Institute for Intelligent Systems…

41 PUBLICATIONS **816** CITATIONS

SEE PROFILE

Biomaterials Science

RSC Publishing

COMMUNICATION

View Article Online
View Journal | View Issue

Dual-responsive drug release from oligonucleotide-capped mesoporous silica nanoparticles†

Cite this: *Biomater. Sci.*, 2013, **1**, 912

Received 9th April 2013,
Accepted 16th May 2013

DOI: 10.1039/c3bm60090d

www.rsc.org/biomaterialsscience

Xing Ma,[a] Onn Shaun Ong[a] and Yanli Zhao*[a,b]

Mesoporous silica nanoparticles (MSNPs) are functionalized with 15-mer single-stranded DNA (ssDNA). After loading of doxorubicin, functionalized MSNPs are capped with 33-mer complementary ssDNA through the formation of double-stranded DNA. Encapsulated doxorubicin could be released by either thermal-triggered denaturization of the DNA capping chains or redox-induced disulfide bond cleavage. An *in vitro* study shows successful delivery of doxorubicin into HeLa cells.

One major target of drug delivery using nanotechnology is to achieve controlled drug release so as to minimize unwanted side effects.[1–3] Among numerous drug carriers, Mobil Composition of Matter No. 41 (MCM-41)[4] type mesoporous silica nanoparticles (MSNPs) exhibit many advantages over others. Their unique mesoporous structure, including large surface area, high pore volume and narrow mesopore channels, allows the storage of drugs or biomolecules within well-ordered nano-channels, which can be locally released. In addition, easy functionalization of the surface and nano-channels as well as biocompatibility of MSNPs provide the possibility for their application in the biological field, especially for drug delivery.[5–7]

Since achieving controlled drug release from MSNPs becomes a hot research topic,[8,9] the release mechanisms responsive to various stimuli have been designed, which include the changes in temperature[10,11] and pH,[12,13] light irradiation,[14] redox effect,[15] as well as enzymatic action.[16,17] In the design of drug carriers for controlled release, the selection of capping agents plays an essential role. Many capping materials have been chosen for the purpose of blocking drugs within the nanopores, such as iron oxide,[18] cadmium sulphide,[19] gold nanoparticles,[20] polymers,[21] and proteins.[22] The use of oligonucleotides as functional agents on MSNPs has attracted a lot of attention recently. For example, Climent *et al.*[23] capped the mesopores with single-stranded DNA (ssDNA) through the electrostatic attraction between negatively charged ssDNA and positively charged aminopropyl groups functionalized onto the surface of MSNPs. Chen *et al.*[24] made use of i-motif quadruplex DNA to block the mesopores and realized pH-controlled release based on the morphology change of the DNA chains. Ruiz-Hernandez *et al.*[25] incorporated double-stranded DNA (dsDNA) together with spherical γ-Fe_2O_3 magnetic nanoparticles to cap the mesopores and utilized magnetic field induced heat to trigger the uncapping for drug release. In addition to their biocompatibility, oligonucleotides possess extra biological functions for the drug delivery applications. For instance, oligonucleotides with a specific sequence (aptamer) can be developed to serve as targeting ligands on the nanoparticle surface.[26,27] Short interfering RNA (siRNA) with short RNA chains can be delivered into target cells to silence certain protein expression within cells, achieving an additional gene therapy effect in the cancer treatment.[28] Moreover, most of the current drug/gene co-delivery systems were developed through the electrostatic interactions between negatively charged gene and cationic polymers coated on the MSNP surface.[21,29,30] The drug and gene release from these co-delivery systems was based on the free diffusion after the endocytosis. Zero release before entering into cancer cells and then controlled drug/gene release inside the cancer cells are rather essential for successful cancer treatment. Thus, it is of great significance to develop controlled drug delivery systems using oligonucleotides as capping agents.

Herein, we report a new approach to realize controlled drug release based on oligonucleotide capped MSNPs, which are responsive to both heat and redox changes for drug release (Scheme 1). MSNPs were first functionalized with a disulfide bond containing carboxylic acid groups at the orifice of the mesopores. An amino group modified 15-mer ssDNA was conjugated onto the MSNP surface through amidation between the amino group and carboxylic acid. After drug molecules

[a]*School of Materials Science and Engineering, Nanyang Technological University, 50 Nanyang Avenue, Singapore 639798. E-mail: zhaoyanli@ntu.edu.sg*
[b]*Division of Chemistry and Biological Chemistry, School of Physical and Mathematical Sciences, Nanyang Technological University, 21 Nanyang Link, Singapore 637371*

†Electronic supplementary information (ESI) available. See DOI: 10.1039/c3bm60090d

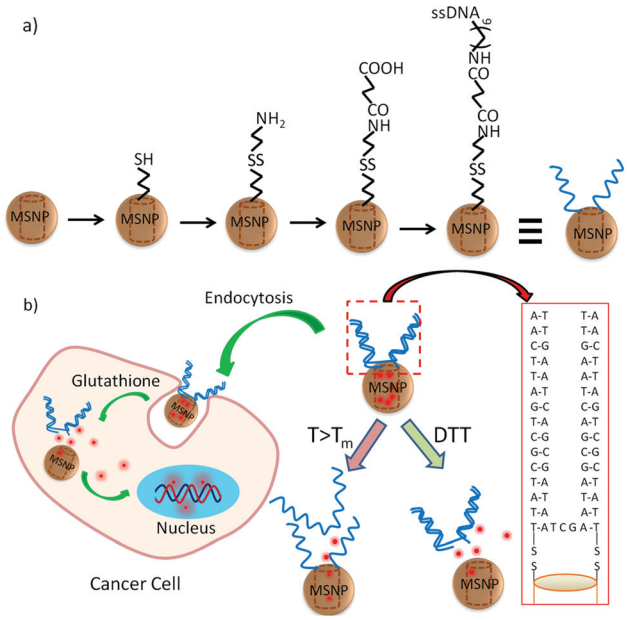

Scheme 1 (a) Synthetic route for the preparation of MSNP–SS–ssDNA, and (b) illustrative mechanism of dual-responsive drug release from oligonucleotide capped MSNPs.

were loaded into the mesopores of functional MSNPs, long 33-mer complementary ssDNA (cDNA) was introduced to hybridize with short 15-mer ssDNA functionalized on the MSNP surface, blocking the loaded drugs within the mesopores. Controlled drug release can be achieved either by heat triggered denaturization of the dsDNA chains, or by the introduction of a reducing agent, such as dithiothreitol (DTT) and glutathione (GSH), to cleave the pre-installed disulfide bond connected between dsDNA and MSNPs. Different from other reported oligonucleotide-containing systems,[23–25] the present dual-responsive delivery system may allow for multiple applications. For example, in the case of extracellular drug delivery for the therapy of some skin diseases, the MSNP based drug delivery system as a drug reservoir within the tissue matrix could initially hold the drug inside the mesopores under normal conditions. External heat could then be applied on-demand to trigger localized drug release from MSNPs for therapy. In the case of intracellular drug delivery for cancer therapy, once the delivery system is internalized into cancer cells through endocytosis, the intracellular presence of a natural reducing agent, GSH,[31] would automatically trigger the drug release by the cleavage of the disulfide bond.[32–34]

MSNPs were synthesized by a conventional sol–gel process in base solution, and thiol groups were then functionalized onto the outside surface of MSNPs through the grafting method. After the removal of the surfactant cetyltrimethylammonium bromide (CTAB), thiol group (–SH) modified MSNPs, denoted as MSNP–SH, were produced. The obtained MSNP–SH was characterized by Transmission Electron Microscopy (TEM), as shown in Fig. 1. The average diameter of MSNP–SH was estimated to be 165 nm by randomly counting 30 nanoparticles in Fig. 1a. The mesoporous structure and uniform nanopores are clearly observed (Fig. 1b). Brunauer–Emmett–Teller (BET) N_2 adsorption/desorption measurement shows a typical type IV isotherm, indicative of a mesoporous structure. The BET surface area was determined to be 808.8 ± 4.8 $m^2\ g^{-1}$ and the pore volume was found to be 0.78 $cm^3\ g^{-1}$ (Table S1 in the ESI†). Barrett–Joyner–Halenda (BJH) pore size distribution sharply focuses on 2.8 nm (Fig. S1 in the ESI†). The characteristic peak (001) at $2\theta = 2.2°$ in the powder X-ray diffraction pattern of MSNP–SH certifies the formation of MCM-41 type MSNPs (Fig. S2 in the ESI†).[35]

Then, MSNP–SH reacted with *S*-(2-aminoethylthio)-2-thiopyridine hydrochloride that was prepared according to a previous report,[36] to form disulfide bond containing amino group functionalized MSNPs, denoted as MSNP–SS–NH_2. A terminal carboxylic acid group was introduced by reacting MSNP–SS–NH_2 with succinic anhydride in DMF in the presence of triethylamine (TEA), resulting in MSNP–SS–COOH. The functionalization process was traced by FT-IR spectra as well as zeta-potential measurements. In addition, bare MSNPs without any modifications were prepared as control. The appearance of a minor peak at 2560 cm^{-1} in the FT-IR spectrum of MSNP–SH indicates successful grafting of thiol groups onto the MSNP surface (Fig. 2). Then, the peak at 2560 cm^{-1} disappeared, and new peaks around 1513 cm^{-1} were observed, on account of the introduction of amine groups on the surface, indicating the formation of a disulfide bond containing an amine group in MSNP–SS–NH_2. Further introduction of a carboxylic acid group on MSNP–SS–COOH was confirmed by an obvious peak at 1726 cm^{-1} attributed to the –COOH group, and by another new peak at 1560 cm^{-1} due to the N–H stretching in the amide bond.[37] Except for the bare MSNPs, all other samples have the peak at 2930 cm^{-1}, which is assigned to the $-CH_2$ stretching in the alkyl chains of functional groups. The zeta-potential value of MSNP–SH was reversed from a negative value of −24.8 mV to a positive one of 44.2 mV after the formation of MSNP–SS–NH_2, because of the amine groups in MSNP–SS–NH_2 (Table S2 in the ESI†). After the introduction of a carboxylic acid group, the zeta-potential value was reversed again to a negative value of −45.9 mV, further supporting the observations from the FT-IR spectra and proving the successful functionalization process.

An amino group modified 15-mer ssDNA was conjugated onto the MSNP surface by reacting it with the carboxylic acid group of MSNP–SS–COOH to form amide bond linkage, and the formed nanoparticles are denoted as MSNP–SS–ssDNA. After the reaction, the product was collected by centrifugation and washed with PBS (phosphate buffered saline) buffer twice. Then, MSNP–SS–ssDNA was suspended in PBS buffer for the measurement of the UV-vis spectrum. The absorbance peak at 260 nm indicating the presence of oligonucleotides was observed in the spectrum (Fig. 1d). In addition, the surface DNA chains can be visualized in the TEM image, indicated by small red arrows (Fig. 1c). In order to prove that the 33-mer complementary ssDNA (cDNA) chain can hybridize with the 15-mer ssDNA chain on the MSNP surface, Cy5 dye labeled 33-mer cDNA (cDNA/Cy5) was used to react with MSNP–SS–

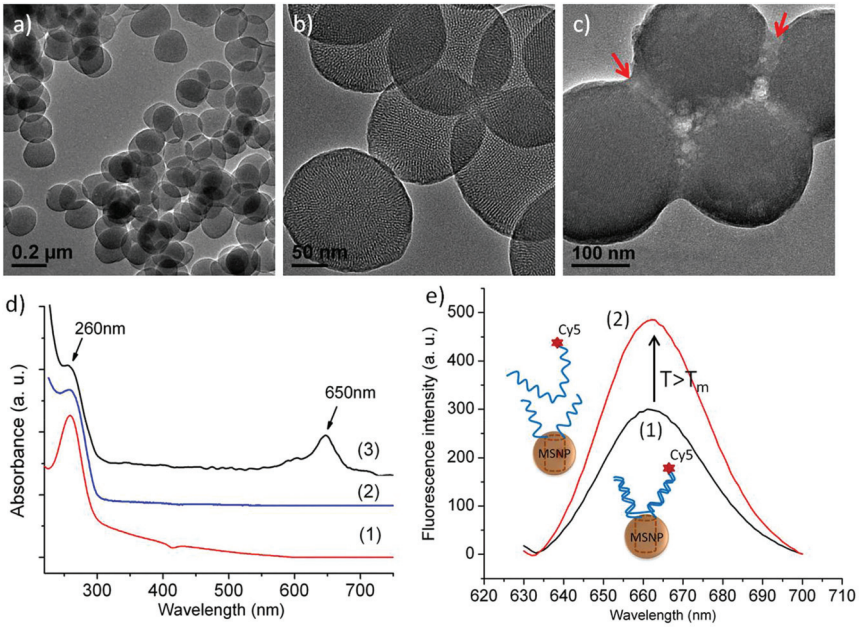

Fig. 1 TEM images of MSNP–SH (a) at low magnification and (b) at high magnification, and (c) FITC-loaded MSNP–SS–ssDNA. (d) UV-vis spectra of (d-1) ssDNA, (d-2) MSNP–SS–ssDNA, and (d-3) MSNP–SS–dsDNA/Cy5. (e) Fluorescence spectra of the MSNP–SS–dsDNA/Cy5 solution (e-1) before and (e-2) after thermal-triggered denaturization ($T > T_m$).

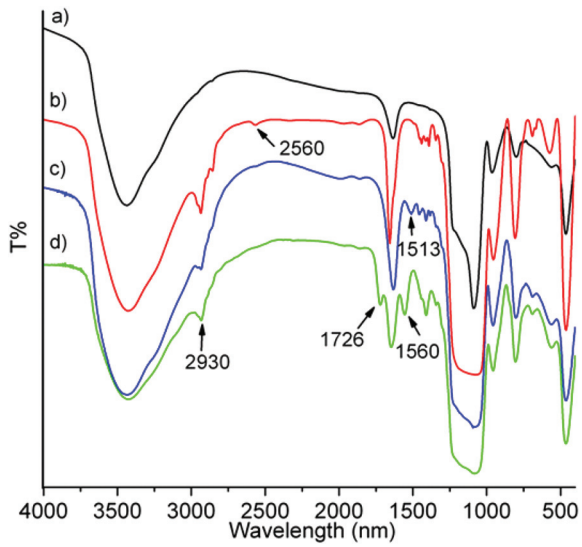

Fig. 2 FT-IR spectra of (a) bare MSNPs, (b) MSNP–SH, (c) MSNP–SS–NH_2, and (d) MSNP–SS–COOH.

ssDNA, and the hybridization was taking place in Tris–EDTA buffer (pH = 8.0) at room temperature under mild stirring for 1 hour. Then, the formed dsDNA/Cy5 capped MSNPs, denoted as MSNP–SS–dsDNA/Cy5, were collected by centrifugation and washed with PBS twice before the UV-vis measurement. In addition to the peak at 260 nm for the DNA unit, an extra peak at 650 nm from Cy5 dye was found in the UV-vis spectrum of MSNP–SS–dsDNA/Cy5, demonstrating successful hybridization between the complementary DNA chain and ssDNA chain on the MSNP surface (Fig. 1d). After heat treatment for 15 min at 60 °C, higher than the melting temperature of dsDNA (T_m = 40.3 °C), the fluorescence intensity at 661 nm (excited by 620 nm) for Cy5 dye in the MSNP–SS–dsDNA/Cy5 solution was greatly enhanced (Fig. 1e). This change means that the denaturization of dsDNA on the MSNP surface occurred, leading to the release of a Cy5 labeled complementary ssDNA chain.

To investigate the controlled release mechanism of oligonucleotide capped MSNPs, fluorescein isothiocyanate (FITC) was loaded into the mesopores by suspending MSNP–SS–ssDNA in saturated FITC aqueous solution under continuous stirring for 24 h. Then, 33-mer complementary ssDNA was added to hybridize with 15-mer ssDNA on the MSNP surface, so as to cap the mesopores and block loaded FITC inside the mesopores. After capping, FITC loaded oligonucleotide capped MSNPs, denoted as FITC-loaded MSNP–SS–dsDNA, were collected by centrifugation and washed with Tris–EDTA buffer (pH = 8.0) in order to remove unloaded FITC. A stimulus-responsive release profile was obtained by monitoring the fluorescence intensity of FITC at 526 nm (excited by 488 nm) from the supernatant of the FITC-loaded MSNP–SS–dsDNA solution over time.

Without any stimulus, a negligible amount of FITC was released at room temperature, indicating effective capping by the hybridization of 33-mer complementary ssDNA with 15-mer ssDNA on the MSNP surface (Fig. 3a-3). Upon the addition of reducing agent DTT, a large amount of FITC was released with a sharp releasing profile (Fig. 3a-1). It can be anticipated that the disulfide bond connected between dsDNA and MSNPs was effectively cleaved by reducing agent DTT, and the dsDNA was removed from the MSNP surface, leading to the uncapping of mesopores. As only thiol group (–SH) was left on the mesopore orifice, FITC could be released without any blocking.

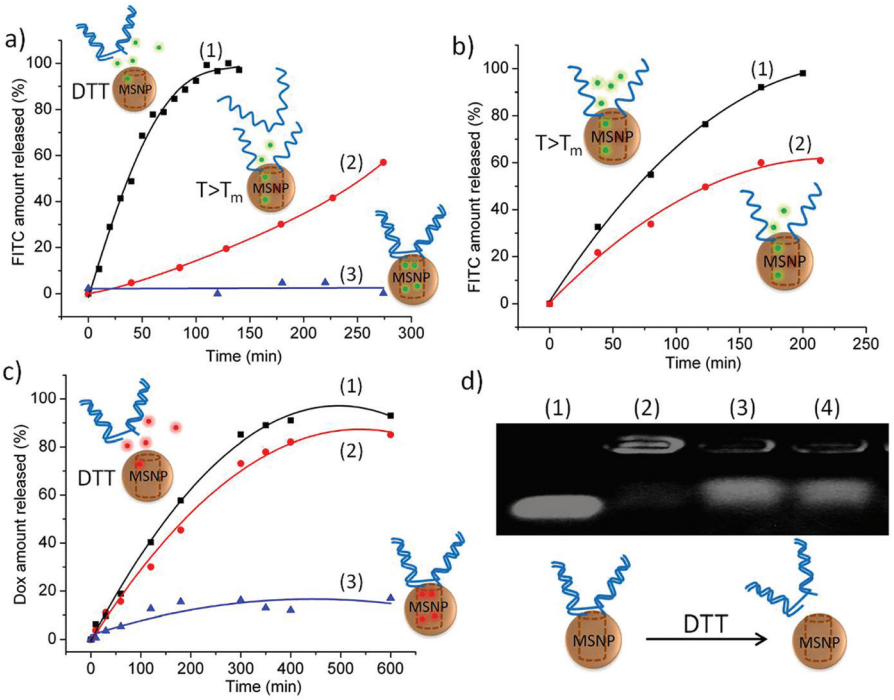

Fig. 3 (a) Stimulus-responsive FITC release profiles from FITC-loaded MSNP–SS–dsDNA under the conditions of (a-1) addition of 25 mM DTT, (a-2) 45 °C thermal treatment, and (a-3) control. (b) FITC release profiles from FITC-loaded MSNP–SS–ssDNA without cDNA capping (b-1) at 45 °C and (b-2) at room temperature. (c) Dox release profiles from Dox-loaded MSNP–SS–dsDNA with (c-1) 20 mM DTT, (c-2) 10 mM DTT, and (c-3) control. (d) Agarose gel electrophoresis: lanes from left to right are (d-1) free ssDNA, (d-2) MSNP–SS–dsDNA, (d-3) MSNP–SS–dsDNA with 20 mM DTT, and (d-4) MSNP–SS–dsDNA with 10 mM DTT.

In addition to redox-responsive release, we also investigated the thermal-triggered release. When the temperature was kept at 45 °C, higher than the melting temperature (T_m = 40.3 °C) of the hybridized dsDNA, continuous release of FITC was observed with an increased releasing rate (Fig. 3a-2). In the case of thermal-triggered release, the relatively less released amount of FITC than that treated with DTT could be explained by the partial blocking effect of residual ssDNA on the MSNP surface. As the denaturization of dsDNA was taking place over time, more and more mesopores were opened gradually, showing an inverse parabolic release curve.[25] As a control, the FITC release profiles from FITC-loaded MSNP–SS–ssDNA without any complementary ssDNA capping were recorded both at room temperature and under 45 °C (Fig. 3b). With increasing time, both release profiles exhibit typical free diffusion character with parabolic release curves, because the release rate is dependent on the difference of cargo concentrations inside and outside mesopores. In these cases, it is reasonable to observe a quicker release rate and a higher FITC release amount when increasing the temperature (45 °C), as the free diffusion rate is also temperature-dependent.

Agarose gel electrophoresis not only confirms the successful conjugation and hybridization of dsDNA on the MSNP surface, but also certifies the uncapping of dsDNA by disulfide bond cleavage (Fig. 3d). Free ssDNA shifted down freely in the first lane, while DNA in MSNP–SS–dsDNA was retained inside the well without any shifting in the second lane, indicated by a strong bright band in the well. After the addition of reducing agent DTT, the DNA band shifted down again in the third and fourth lanes, implying that the disulfide bond cleavage led to the DNA release from the MSNP surface.

Taking account of further applications of the system for *in vitro* drug delivery, anticancer drug doxorubicin (Dox) was loaded into MSNP–SS–ssDNA and capped by 33-mer complementary ssDNA through a similar method. Then, we investigated redox-responsive Dox release from Dox-loaded MSNP–SS–dsDNA. Less than 10% Dox was released from the nanoparticles after 10 hour incubation without the addition of any reducing agent, indicating the efficient capping effect of the dsDNA. Upon the addition of DTT, significant Dox release was observed (Fig. 3c). When increasing the DTT amount, a quicker releasing rate was recorded, further supporting the disulfide bond cleavage based release mechanism. Similar release profiles were also observed when using GSH as a reducing agent. According to previous reports,[32–34] disulfide bonds could be effectively cleaved when exposed to a high GSH concentration within the intracellular environment. Thus, we further conducted *in vitro* drug delivery of the system using HeLa cell lines.

To trace the location of MSNPs *in vitro*, FITC labeled MSNPs, denoted as MSNP(FITC), were prepared and used for the studies of cellular uptake and *in vitro* drug delivery. After being incubated with 20 μg mL^{-1} Dox-loaded MSNP(FITC)–SS–dsDNA for 24 h, HeLa cells were washed with PBS three times in order to remove free nanoparticles not taken by the cells. Then, the cells were fixed with polyformaldehyde, and the cell

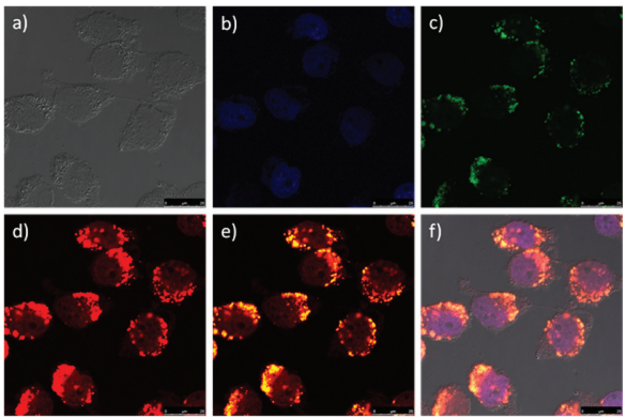

Fig. 4 CLSM images of HeLa cells after treatment with 20 μg mL^{-1} Dox-loaded MSNP(FITC)–SS–dsDNA for 24 h with (a) bright field, (b) DAPI channel (405/450 ± 10 nm), (c) FITC channel (488/525 ± 10 nm), (d) Dox channel (488/585 ± 10 nm), (e) merged from FITC and Dox channels, and (f) merged from bright field, DAPI, FITC, and Dox channels. Scale bar: 25 μm.

nucleus was stained by 4′,6-diamidino-2-phenylindole (DAPI) before observation with confocal laser scanning microscopy (CLSM). Green color dots from MSNP(FITC) were only observed inside cells surrounding the cell nucleus that was stained in blue color by DAPI (Fig. 4b and c). No green dots were observed outside the cells, suggesting effective cellular uptake of MSNP(FITC) through endocytosis. Furthermore, flow cytometry analysis confirmed the cellular uptake of MSNP(FITC)–SS–dsDNA (Fig. S3 in the ESI†). The histogram (green curve) for HeLa cells treated with MSNP(FITC)–SS–dsDNA right-shifted with high FITC fluorescence intensity, as compared to that of the control without any treatment (red curve). The Dox release inside cells was clearly observed, as red fluorescence color from Dox was found outside the locations of the nanoparticles. Extra red color can be seen beyond the bright yellow dots that are generated by the overlay of FITC (green) and Dox (red) channels (Fig. 4e). The red color from the nucleus indicates that Dox was released from MSNP(FITC) and was further diffused into the nucleus where Dox interacts with DNA to induce the apoptosis (Fig. 4f).[38] The CLSM results confirmed that Dox could be released from MSNP(FITC)–SS–dsDNA inside the cancer cells. According to the controlled release mechanism (Fig. 3c), the intracellular drug release can be explained by intracellular GSH triggered disulfide bond cleavage, leading to the Dox release from the mesopores of MSNPs within the cancer cells.

The cytotoxicity assay was performed to evaluate the anticancer efficacy of the drug delivery system. In order to prove that the cell death was really caused by the delivered Dox instead of the toxic effect from the MSNP based carrier, the cytotoxicity effect of MSNP–SS–dsDNA was evaluated as well. Without the Dox loading, the relative cell viability of HeLa cells after 24 h incubation with MSNP–SS–dsDNA maintains a high value (about 75%) even under the highest concentration (200 μg mL^{-1}) of MSNP–SS–dsDNA used (Fig. 5a-1). For another group (Fig. 5a-2), after 24 h incubation with MSNP–

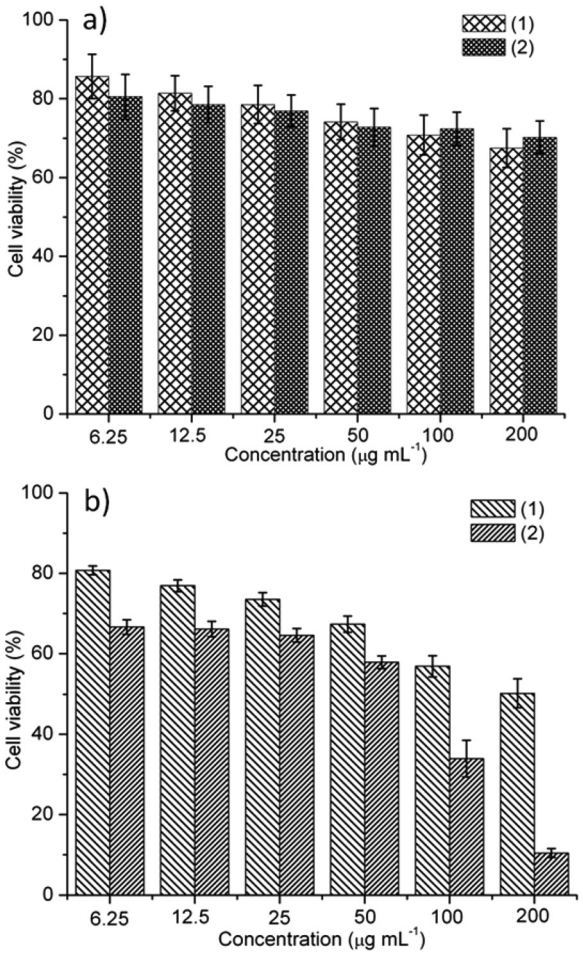

Fig. 5 Relative cell viability of HeLa cells after treatment with (a) MSNP–SS–dsDNA or (b) Dox-loaded MSNP–SS–dsDNA for 24 h. For (a-1) and (b-1), the MTT assay was conducted right after the 24 h incubation with corresponding nanoparticles. For (a-2) and (b-2), the medium was replaced with new medium after 24 h incubation with corresponding nanoparticles, and the cells were cultured for another 24 h before the MTT assay.

SS–dsDNA, the culture medium was replaced with new medium. Another 24 h incubation did not decrease the cell viability. Instead, a slight increase of the cell viability was found, which suggests that the delivery carrier MSNP–SS–dsDNA has a negligible cytotoxic effect on HeLa cells. After being incubated with Dox-loaded MSNP–SS–dsDNA for 24 h, however, the cell viability was decreased obviously (Fig. 5b-1). For another group (Fig. 5b-2), after 24 h incubation with Dox-loaded MSNP–SS–dsDNA, the culture medium was replaced with new medium, and the cells were then incubated for another 24 h. Interestingly, much lower cell viability was observed after the extra 24 h incubation, as the cell viability was decreased from 50% (Fig. 5b-1) to around 10% (Fig. 5b-2) at the concentration of 200 μg mL^{-1} used. These observations firmly support the controlled release of Dox, which induces cell apoptosis and consequently cell death. The Dox release process takes considerable time, *i.e.*, about 10 hours to release about 85% of Dox in the presence of 10 mM DTT. Thus, an even slower release rate inside cells can be expected, since the

reducing capability of GSH is less than that of DTT. In addition, the apoptosis process of the cells will also take some time, finally leading to the cell death. Therefore, higher cytotoxicity was observed after the extra 24 h incubation, demonstrating the high efficacy of the controlled drug delivery system with oligonucleotides as capping agents.

In summary, we have designed and fabricated a controlled drug delivery system based on mesoporous silica nanoparticles (MSNPs) capped with cleavable oligonucleotides. A dual-responsive drug release mechanism has been demonstrated, either by thermal-triggered denaturization of a double stranded DNA capping agent, or by redox-induced disulfide bond cleavage. An *in vitro* study shows effective cellular uptake of oligonucleotide capped MSNPs and successful doxorubicin release within HeLa cancer cells. Negligible cytotoxicity of the MSNP carrier has been observed, while a high efficacy of cell death has been achieved by delivering doxorubicin into cancer cells. Considering the biological function of oligonucleotides under exploration, as well as localized thermal-responsive drug release for non-invasive control, we can expect even more promising applications of the oligonucleotide capped MSNPs in the disease treatment.

This work was financially supported by the Singapore National Research Foundation Fellowship (NRF2009NRF-RF001-015), the Singapore National Research Foundation CREATE program – Singapore Peking University Research Centre for a Sustainable Low-Carbon Future, and the Centre of Excellence for Silicon Technologies (A*Star SERC no. 112 351 0003).

Notes and references

1 O. C. Farokhzad and R. Langer, *ACS Nano*, 2009, **3**, 16–20.
2 G. A. Hughes, *Nanomedicine*, 2005, **1**, 22–30.
3 O. M. Koo, I. Rubinstein and H. Onyuksel, *Nanomedicine*, 2005, **1**, 193–212.
4 C. T. Kresge, M. E. Leonowicz, W. J. Roth, J. C. Vartuli and J. S. Beck, *Nature*, 1992, **359**, 710–712.
5 K. K. Coti, M. E. Belowich, M. Liong, M. W. Ambrogio, Y. A. Lau, H. A. Khatib, J. I. Zink, N. M. Khashab and J. F. Stoddart, *Nanoscale*, 2009, **1**, 16–39.
6 A. Popat, S. B. Hartono, F. Stahr, J. Liu, S. Z. Qiao and G. Q. Lu, *Nanoscale*, 2011, **3**, 2801–2818.
7 F. Tang, L. Li and D. Chen, *Adv. Mater.*, 2012, **24**, 1504–1534.
8 J. L. Vivero-Escoto, I. I. Slowing, B. G. Trewyn and V. S. Y. Lin, *Small*, 2010, **6**, 1952–1967.
9 I. I. Slowing, J. L. Vivero-Escoto, C.-W. Wu and V. S. Y. Lin, *Adv. Drug Delivery Rev.*, 2008, **60**, 1278–1288.
10 J.-H. Park, Y.-H. Lee and S.-G. Oh, *Macromol. Chem. Phys.*, 2007, **208**, 2419–2427.
11 P.-W. Chung, R. Kumar, M. Pruski and V. S. Y. Lin, *Adv. Funct. Mater.*, 2008, **18**, 1390–1398.
12 Y. L. Zhao, Z. Li, S. Kabehie, Y. Y. Botros, J. F. Stoddart and J. I. Zink, *J. Am. Chem. Soc.*, 2010, **132**, 13016–13025.
13 H. P. Rim, K. H. Min, H. J. Lee, S. Y. Jeong and S. C. Lee, *Angew. Chem., Int. Ed.*, 2011, **50**, 8853–8857.
14 H. Yan, C. Teh, S. Sreejith, L. Zhu, A. Kwok, W. Fang, X. Ma, K. T. Nguyen, V. Korzh and Y. L. Zhao, *Angew. Chem., Int. Ed.*, 2012, **51**, 8373–8377.
15 T. D. Nguyen, H.-R. Tseng, P. C. Celestre, A. H. Flood, Y. Liu, J. F. Stoddart and J. I. Zink, *Proc. Natl. Acad. Sci. U. S. A.*, 2005, **102**, 10029–10034.
16 A. Bernardos, E. Aznar, M. D. Marcos, R. Martínez-Máñez, F. Sancenón, J. Soto, J. M. Barat and P. Amorós, *Angew. Chem., Int. Ed.*, 2009, **48**, 5884–5887.
17 C. Park, H. Kim, S. Kim and C. Kim, *J. Am. Chem. Soc.*, 2009, **131**, 16614–16615.
18 S. Giri, B. G. Trewyn, M. P. Stellmaker and V. S. Y. Lin, *Angew. Chem., Int. Ed.*, 2005, **44**, 5038–5044.
19 C.-Y. Lai, B. G. Trewyn, D. M. Jeftinija, K. Jeftinija, S. Xu, S. Jeftinija and V. S. Y. Lin, *J. Am. Chem. Soc.*, 2003, **125**, 4451–4459.
20 C.-L. Zhu, C.-H. Lu, X.-Y. Song, H.-H. Yang and X.-R. Wang, *J. Am. Chem. Soc.*, 2011, **133**, 1278–1281.
21 D. R. Radu, C.-Y. Lai, K. Jeftinija, E. W. Rowe, S. Jeftinija and V. S. Y. Lin, *J. Am. Chem. Soc.*, 2004, **126**, 13216–13217.
22 Z. Luo, K. Cai, Y. Hu, L. Zhao, P. Liu, L. Duan and W. Yang, *Angew. Chem., Int. Ed.*, 2011, **50**, 640–643.
23 E. Climent, R. Martínez-Máñez, F. Sancenón, M. D. Marcos, J. Soto, A. Maquieira and P. Amorós, *Angew. Chem., Int. Ed.*, 2010, **49**, 7281–7283.
24 C. Chen, F. Pu, Z. Huang, Z. Liu, J. Ren and X. Qu, *Nucleic Acids Res.*, 2011, **39**, 1638–1644.
25 E. Ruiz-Hernández, A. Baeza and M. Vallet-Regí, *ACS Nano*, 2011, **5**, 1259–1266.
26 L. Cerchia and V. de Franciscis, *Trends Biotechnol.*, 2010, **28**, 517–525.
27 L. Yang, X. Zhang, M. Ye, J. Jiang, R. Yang, T. Fu, Y. Chen, K. Wang, C. Liu and W. Tan, *Adv. Drug Delivery Rev.*, 2011, **63**, 1361–1370.
28 Y.-K. Oh and T. G. Park, *Adv. Drug Delivery Rev.*, 2009, **61**, 850–862.
29 H. Meng, M. Liong, T. Xia, Z. Li, Z. Ji, J. I. Zink and A. E. Nel, *ACS Nano*, 2010, **4**, 4539–4550.
30 A. M. Chen, M. Zhang, D. Wei, D. Stueber, O. Taratula, T. Minko and H. He, *Small*, 2009, **5**, 2673–2677.
31 A. Meister and M. E. Anderson, *Annu. Rev. Biochem.*, 1983, **52**, 711–760.
32 R. Hong, G. Han, J. M. Fernández, B.-J. Kim, N. S. Forbes and V. M. Rotello, *J. Am. Chem. Soc.*, 2006, **128**, 1078–1079.
33 H. Kim, S. Kim, C. Park, H. Lee, H. J. Park and C. Kim, *Adv. Mater.*, 2010, **22**, 4280–4283.
34 Q. Zhang, F. Liu, K. T. Nguyen, X. Ma, X. Wang, B. Xing and Y. L. Zhao, *Adv. Funct. Mater.*, 2012, **22**, 5144–5156.
35 S. Inagaki, S. Guan, T. Ohsuna and O. Terasaki, *Nature*, 2002, **416**, 304–307.
36 Y. W. Ebright, Y. Chen, Y. Kim and R. H. Ebright, *Bioconjugate Chem.*, 1996, **7**, 380–384.
37 C. Park, K. Oh, S. C. Lee and C. Kim, *Angew. Chem., Int. Ed.*, 2007, **46**, 1455–1457.
38 E. J. Gabbay, D. Grier, R. E. Fingerle, R. Reimer, R. Levy, S. W. Pearce and W. D. Wilson, *Biochemistry*, 1976, **15**, 2062–2070.